Noninvasive Assessment of Inspiratory Muscle Neuromechanical Coupling During Inspiratory Threshold Loading

MANUEL LOZANO-GARCÍA[1,2,3], **LUIS ESTRADA-PETROCELLI**[1,2], **(Senior Member, IEEE)**, **JOHN MOXHAM**[4], **GERRARD F. RAFFERTY**[5,6], **ABEL TORRES**[1,2,3], **(Senior Member, IEEE)**, **CAROLINE J. JOLLEY**[5,6,*], **AND RAIMON JANÉ**[1,2,3,*], **(Senior Member, IEEE)**

[1]Institute for Bioengineering of Catalonia (IBEC), The Barcelona Institute of Science and Technology (BIST), 08019 Barcelona, Spain
[2]Biomedical Research Networking Centre in Bioengineering, Biomaterials and Nanomedicine (CIBER-BBN), 28029 Barcelona, Spain
[3]Department of Automatic Control (ESAII), Universitat Politècnica de Catalunya (UPC)-Barcelona Tech, 08019 Barcelona, Spain
[4]Faculty of Life Sciences & Medicine, King's College London, King's Health Partners, London SE1 9RT, U.K.
[5]King's College Hospital NHS Foundation Trust, King's Health Partners, London SE5 9RS, U.K.
[6]Centre for Human & Applied Physiological Sciences, School of Basic & Medical Biosciences, Faculty of Life Sciences & Medicine, King's College London, King's Health Partners, London SE1 9RT, U.K.

Corresponding author: Manuel Lozano-García (mlozano@ibecbarcelona.eu)

*Caroline J. Jolley and Raimon Jané contributed equally to this work.

ABSTRACT Diaphragm neuromechanical coupling (NMC), which reflects the efficiency of conversion of neural activation to transdiaphragmatic pressure (P_{di}), is increasingly recognized to be a useful clinical index of diaphragm function and respiratory mechanics in neuromuscular weakness and cardiorespiratory disease. However, the current gold standard assessment of diaphragm NMC requires invasive measurements of P_{di} and crural diaphragm electromyography ($oesEMG_{di}$), which complicates the measurement of diaphragm NMC in clinical practice. This is the first study to compare invasive measurements of diaphragm NMC (iNMC) using the relationship between P_{di} and $oesEMG_{di}$, with noninvasive assessment of NMC (nNMC) using surface mechanomyography ($sMMG_{lic}$) and electromyography ($sEMG_{lic}$) of lower chest wall inspiratory muscles. Both invasive and noninvasive measurements were recorded in twelve healthy adult subjects during an inspiratory threshold loading protocol. A linear relationship between noninvasive $sMMG_{lic}$ and $sEMG_{lic}$ measurements was found, resulting in little change in nNMC with increasing inspiratory load. By contrast, a curvilinear relationship between invasive P_{di} and $oesEMG_{di}$ measurements was observed, such that there was a progressive increase in iNMC with increasing inspiratory threshold load. Progressive recruitment of lower ribcage muscles, serving to enhance the mechanical advantage of the diaphragm, may explain the more linear relationship between $sMMG_{lic}$ and $sEMG_{lic}$ (both representing lower intercostal plus costal diaphragm activity) than between P_{di} and crural $oesEMG_{di}$. Noninvasive indices of NMC derived from $sEMG_{lic}$ and $sMMG_{lic}$ may prove to be useful indices of lower chest wall inspiratory muscle NMC, particularly in settings that do not have access to invasive measures of diaphragm function.

INDEX TERMS Electromyography, inspiratory threshold loading, mechanomyography, neuromechanical coupling, respiratory muscles.

The associate editor coordinating the review of this manuscript and approving it for publication was Venkata Rajesh Pamula.

I. INTRODUCTION

Accurate assessment of respiratory muscle function is essential for both research and clinical practice [1]. Respiratory

muscle function tests are particularly useful in the assessment of patients with respiratory symptoms [1] and for the diagnosis, phenotyping, and monitoring of patients with neuromuscular disease [2], [3]. The diaphragm is the principal muscle of inspiration [4], [5], and diaphragm weakness may present as breathlessness [6], [7], progressing to respiratory failure when weakness is severe [3]. Unlike electrical activation of the diaphragm, transdiaphragmatic pressure (P_{di}) generation is dependent on neuromechanical coupling (NMC), i.e. the ability of the diaphragm muscle to transform electrical activation into pressure generation [8]. When the diaphragm fails to transform electrical activation into P_{di}, neuromechanical uncoupling occurs. Neuromechanical uncoupling is commonly observed in obstructive lung disease, such as chronic obstructive pulmonary disease, in which the force-generating capacity of the diaphragm is impaired by lung hyperinflation and altered chest wall geometry [9]. Neuromechanical uncoupling has been implicated in the perception of respiratory discomfort (breathlessness) in obstructive lung disease [10], [11] and in neuromuscular disease [12], [13], and is a factor determining successful weaning from mechanical ventilation [14]. Measurements of inspiratory muscle NMC could therefore provide clinically useful indices of inspiratory muscle function.

The gold standard assessment of human diaphragm pressure generation and neural respiratory drive requires invasive procedures, such as the balloon-catheter technique to measure P_{di} [1], and the use of a multipair esophageal electrode catheter to assess neural respiratory drive by quantifying the crural diaphragm electromyogram ($oesEMG_{di}$) [15]. These invasive tests can be uncomfortable for patients, require some skill from the operator involved, and are therefore rarely carried out in clinical practice. The development of novel, noninvasive indices of inspiratory NMC would therefore represent a significant advance in the assessment of patients with disordered respiratory mechanics.

The surface mechanomyogram (sMMG) is a noninvasive measure of muscle surface vibrations due to motor unit mechanical activity [16] and represents the mechanical counterpart of motor unit electrical activity as measured by surface electromyography (sEMG). Surface inspiratory muscle mechanomyographic [17]–[20] and electromyographic [19]–[21] signals can be recorded using lateral chest wall accelerometers and electrodes positioned over the lower intercostal spaces, proximal to the zone of apposition of the diaphragm ($sMMG_{lic}$ and $sEMG_{lic}$ respectively). These signals represent activation of the costal diaphragm [22], and of extradiaphragmatic chest wall and abdominal muscle recruitment [20], [23], [24] when respiratory effort increases [25], [26]. Using fixed sample entropy (fSampEn), an analysis technique which is less influenced by cardiac artefacts than conventional root mean square (RMS), we have nevertheless recently demonstrated strong correlations between P_{di} and $sMMG_{lic}$, and $oesEMG_{di}$ and $sEMG_{lic}$ in healthy subjects during a submaximal inspiratory threshold loading protocol [20]. However, the use of $sEMG_{lic}$ and
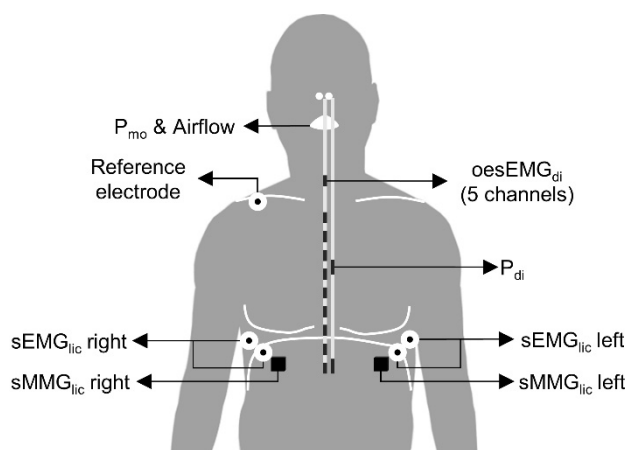

FIGURE 1. Sensor positioning for data acquisition.

$sMMG_{lic}$ to assess NMC of the lower chest wall inspiratory muscles in a wholly noninvasive manner has not previously been investigated.

The principal aim of the study was, therefore, to investigate the combined use of $sEMG_{lic}$ and $sMMG_{lic}$ to calculate lower chest wall inspiratory muscle NMC in a wholly noninvasive manner, in comparison with diaphragm NMC calculated using the invasive $oesEMG_{di}$ and P_{di} measures, in healthy subjects during an incremental inspiratory threshold loading protocol.

II. METHODS
A. ETHICS STATEMENT
This study was approved by the NHS Health Research Authority (NRES Committee London – Dulwich 05/Q0703) and the experiments conformed to the standards of the Declaration of Helsinki. All subjects were fully informed of any risk associated with the study and provided their written consent before participation.

B. DATA ACQUISITION
Both invasive and non-invasive measurements (Fig. 1) of inspiratory muscle activation were recorded at the King's College London Respiratory Physiology Laboratory, King's College Hospital, London, United Kingdom. All signals were acquired from healthy adult subjects, with no history of cardiorespiratory or neuromuscular disease. Some of these signals have been analyzed in a previous study [20].

P_{di} was calculated as the difference between gastric and esophageal pressures recorded using a dual-pressure transducer tipped catheter (CTO-2; Gaeltec Devices Ltd., Dunvegan, UK), as previously described [27], [28]. Crural $oesEMG_{di}$ was recorded using a multipair esophageal electrode catheter (Yinghui Medical Equipment Technology Co. Ltd., Guangzhou, China) [15]. The pressure transducer and electrode catheters were inserted through the nose and optimally positioned as previously described [29], [30]. $sEMG_{lic}$ was recorded bilaterally using two pairs of disposable surface Ag/AgCl electrodes (H124SG; Covidien Kendall) placed on

the skin over the seventh or eighth intercostal spaces, between the mid-axillary and the anterior axillary lines [19]–[21]. $sMMG_{lic}$ was recorded using two triaxial accelerometers (TSD109C2; BIOPAC Systems Inc, CA, USA) attached bilaterally to the skin with adhesive rings as close as possible to the $sEMG_{lic}$ electrodes along the seventh or eighth intercostal space, over the anterior axillary line [17], [20]. Respiratory flow was measured using a pneumotachograph (4830; Hans Rudolph Inc, KS, USA) connected to a differential pressure transducer (DP45; Validyne Engineering, CA, USA). Mouth pressure (P_{mo}) was measured from a side port on the pneumotachograph using a second differential pressure transducer (MP45; Validyne Engineering, CA, USA).

The $oesEMG_{di}$ and $sEMG_{lic}$ signals were amplified (gain 100), high-pass filtered at 10 Hz, and AC-coupled before acquisition (CED 1902; Cambridge Electronic Design Limited, Cambridge, UK). All signals were acquired using a 16-bit analogue-to-digital converter (PowerLab 16/35; ADInstruments Ltd, Oxford, UK) and displayed on a laptop computer running LabChart software (Version 7.2, ADInstruments Pty, Colorado Springs, USA) with analogue to digital sampling at 100 Hz (flow and pressures), 2000 Hz ($sMMG_{lic}$), and 4000 Hz ($oesEMG_{di}$ and $sEMG_{lic}$).

C. PROTOCOL
1) MAXIMAL VOLITIONAL MANEUVERS
Two maximal volitional inspiratory maneuvers were performed initially: maximal inspiratory effort against an occluded mouthpiece (a Mueller maneuver) from functional residual capacity to determine maximal inspiratory mouth pressure (PImax) [1], and maximal inspiration to total lung capacity [30], [31]. These maneuvers were performed sitting upright in a chair with a noseclip in place and were repeated several times to ensure maximal volitional effort. All measurements were recorded continuously during the maneuvers. Each participant's PImax was used to determine the inspiratory threshold loads used in their individual incremental inspiratory threshold loading protocol.

2) INSPIRATORY THRESHOLD LOADING PROTOCOL
All participants performed an inspiratory threshold loading protocol at five inspiratory threshold loads set at 12% (L_1), 24% (L_2), 36% (L_3), 48% (L_4), and 60% (L_5) of the subject's PImax. Inspiratory threshold loads were generated using an electronic inspiratory muscle trainer (POWERbreathe K5; POWERbreathe International Ltd, Southam, UK) attached to the distal end of the pneumotachograph. Subjects were seated and breathed through the pneumotachograph via a mouthpiece with a noseclip in place. Baseline measurements were recorded during a minimum of 2 minutes of quiet tidal breathing (L_0), following which the inspiratory muscle trainer was attached to the pneumotachograph and the series of threshold loads was imposed. Subjects were not provided with any specific instructions to adopt a certain duty cycle and were free to choose their own breathing frequency. Subjects were,

however, informed that effort was needed to overcome the threshold loads, and they were therefore encouraged to focus on using their diaphragm, to perform quick deep inspirations and to ensure that expiration was complete before making their next inspiratory effort. Each load consisted of 30 breaths at most followed by a resting period to allow all respiratory measures to return to baseline.

## D. DATA ANALYSIS
1) DATA PRE-PROCESSING
LabChart data were exported as Matlab files, and analyzed offline in MATLAB (The MathWorks, Inc., vR2014a, Natick, MA, USA).

$oesEMG_{di}$ and $sEMG_{lic}$ signals were resampled at 2000 Hz and filtered with an 8th-order zero-phase Butterworth band-pass filter between 10 and 600 Hz, and with a 2-Hz bandwidth notching comb filter to remove the power line interference at 50 Hz and all its harmonics. $sMMG_{lic}$ signals were resampled at 500 Hz and filtered with an 8th-order zero-phase Butterworth band-pass filter between 5 and 40 Hz. After filtering, the total acceleration measured by each accelerometer ($|sMMG_{lic}|$) was arithmetically calculated as the norm of the vector formed by its three $sMMG_{lic}$ components ($sMMG_{lic}$ X, $sMMG_{lic}$ Y, and $sMMG_{lic}$ Z). P_{mo} and PImax were expressed as absolute values.

All signals were segmented into inspiratory and expiratory signal segments by means of a zero-crossing detector on the P_{mo} signal. After segmentation, all signal segments were visually inspected and those either containing artefacts within the EMG and MMG signals or having an unusual pressure pattern were rejected. In general, less than 30% of respiratory cycles per load were rejected, and these typically occurred at the beginning and the end of each load. The following parameters were then calculated for each respiratory cycle: inspiratory time, duty cycle (inspiratory time / total breathing cycle time), breathing frequency, and inspiratory volume. Inspiratory volume was calculated as the area under the curve of the inspiratory flow trace. The median values of all respiratory cycles during resting breathing and threshold loading were then calculated and ten cycles that contained the four parameters nearest to the median values were automatically selected, resulting in a total of sixty respiratory cycles for each subject.

2) MYOGRAPHIC SIGNAL ANALYSIS USING fSampEn
Sample entropy is a measure of regularity and complexity of time-series signals [32], so that more regular signals are less complex and lead to lower values of sample entropy. The following parameters must be fixed in sample entropy: the embedded dimension, m, and the tolerance, r. The latter is usually set as a percentage of the standard deviation of the signal analyzed. In fSampEn, however, sample entropy is calculated within a moving window, instead of over a whole signal, using a fixed r value for all windows. In this way,
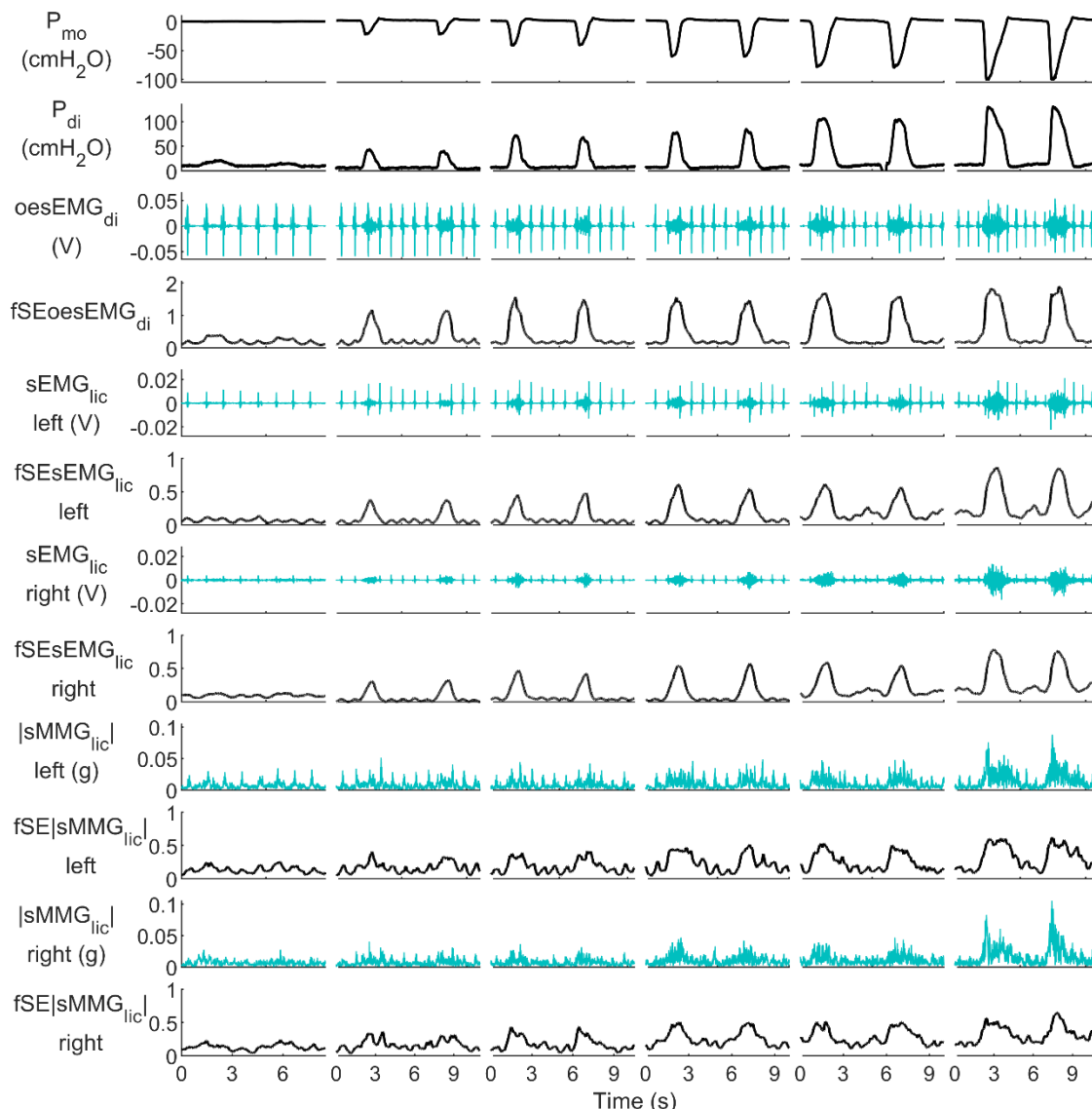
FIGURE 2. Signals recorded during the inspiratory threshold loading protocol in a single healthy subject. Two respiratory cycles are shown during quiet resting breathing, and during inspiratory threshold loading at 12%, 24%, 36%, 48%, and 60% of PImax. The oesEMG$_{di}$ signal shown is the signal recorded from electrode pair 1.

fSampEn is not only sensitive to changes in signal complexity, but also to changes in signal amplitude [33].

In myographic respiratory signals, fSampEn has proven to be less sensitive in quantifying amplitude variations of more deterministic signal components, such as cardiac artefacts, than in quantifying amplitude variations of more complex signal components, such as inspiratory muscle EMG and MMG [21], [33].

In this study, fSampEn signals were calculated for the oesEMG$_{di}$ (fSEoesEMG$_{di}$), sEMG$_{lic}$ (fSEsEMG$_{lic}$), and |sMMG$_{lic}$| (fSE|sMMG$_{lic}$|) signals (Fig. 2), using a moving window of 500 ms with a 50-ms step, m equal to 2 and r equal to 0.05 (fSEoesEMG$_{di}$), 0.3 (fSEsEMG$_{lic}$), and 0.5 (fSE|sMMG$_{lic}$|) times the global standard deviation of each signal. These are the optimal general fSampEn parameters

for inspiratory muscle activity estimation as we previously described [34].

The level of inspiratory muscle activity during each respiratory cycle was calculated as the mean inspiratory P$_{di}$, fSEoesEMG$_{di}$, fSEsEMG$_{lic}$, and fSE|sMMG$_{lic}$| signals. For fSEoesEMG$_{di}$, the highest mean value obtained across all five bipolar electrode pairs was selected. Mean P$_{di}$ was calculated after removal of the baseline from the P$_{di}$ signal, which was determined as the moving minimum using a moving window of 1.5 times the maximum inspiratory time of each load.

The per-breath mean values of P$_{di}$, fSEoesEMG$_{di}$, fSEsEMG$_{lic}$, and fSE|sMMG$_{lic}$| signals were expressed as percentages of their respective largest mean values obtained throughout the inspiratory threshold loading protocol and the two maximal volitional

maneuvers ($P_{di\%max}$, $fSEoesEMG_{di\%max}$, $fSEsEMG_{lic\%max}$, and $fSE|sMMG_{lic}|_{\%max}$).

3) INSPIRATORY MUSCLE NMC

Inspiratory muscle NMC was calculated as the ratio of a mechanical measure ($P_{di\%max}$ or $fSE|sMMG_{lic}|_{\%max}$) to an electrical measure ($fSEoesEMG_{di\%max}$ or $fSEsEMG_{lic\%max}$). Depending on the measures involved, an invasive NMC (iNMC), mixed NMC (mNMC), or noninvasive NMC (nNMC) was calculated as in (1), (2), and (3), respectively.

$$iNMC_{L_i} = \frac{\overline{P_{di\%\,max\,-L_i}}}{\overline{fSEoesEMG_{di\%\,max\,-L_i}}} \quad (1)$$

$$mNMC_{L_i} = \frac{\overline{P_{di\%\,max\,-L_i}}}{\overline{fSEsEMG_{lic\%\,max\,-L_i}}} \quad (2)$$

$$nNMC_{L_i} = \frac{\overline{fSE\,|sMMG_{lic}|_{\%\,max\,-L_i}}}{\overline{fSEsEMG_{lic\%\,max\,-L_i}}} \quad (3)$$

where i goes from 0 to 5, and the overlines represent the average value of the ten respiratory cycles selected for resting breathing and each load.

E. STATISTICAL ANALYSIS

Normality of all measures and parameters calculated for each subject was tested using Lilliefors tests. Since not all measures and parameters had a normal distribution, all data are expressed as median and interquartile range.

Changes in inspiratory and expiratory times, duty cycle, respiratory frequency, and inspiratory volume during threshold loading were assessed using Friedman tests and multiple Wilcoxon signed-rank tests with Bonferroni adjusted p-values.

Linear relationships between measures of inspiratory muscle activity could not be assumed a priori, and therefore the relationships between electrical and mechanical measures during threshold loading were assessed individually using Spearman's rank correlation coefficients (ρ).

Changes in iNMC, mNMCs, and nNMCs during threshold loads L1-L5 were firstly assessed for the 12 subjects using Friedman tests, followed by multiple Wilcoxon signed-rank tests with Bonferroni adjustment for multiple comparisons. Secondly, linear regression analysis was used individually to assess whether iNMC, mNMCs, and nNMCs increased significantly during threshold loads L1-L5.

The significance level for all statistical tests was set at 0.05.

III. RESULTS

Twelve subjects (6 male and 6 female, age 33 (30-39) years, body mass index 22.2 (20.6-24.2) kg/m^2, forced expiratory volume in 1 second 98.0 (94.8-105.5) % of predicted, forced vital capacity 105.0 (91.5-110.2) % of predicted, forced expiratory volume in 1 second/forced vital capacity 81.9 (74.1-83.9) %) were included in the study and completed the incremental inspiratory loading protocol.

A. BREATHING PATTERN AND PRESSURE GENERATION

The group median (interquartile range) PImax was 87.0 (78.0-116.5) cmH$_2$O. The inspiratory threshold loads increased from 11 (10-14) cmH$_2$O during L1 to 52 (47-70) cmH$_2$O during L5. P_{mo} decreased from 0.3 (0.3-0.4) cmH$_2$O during L0 to 53.7 (49.5-68.4) cmH$_2$O (p < 0.001) during L5. P_{di} increased from 11.1 (7.1-11.7) cmH$_2$O at rest to 64.4 (46.1-67.9) cmH$_2$O (p < 0.001) at L5. Evolution of inspiratory time, duty cycle, respiratory frequency, and inspiratory volume during threshold loading is shown in Fig. 3. No significant differences were found in inspiratory time, duty cycle, and respiratory frequency during the inspiratory threshold loading protocol. Significant differences were found in expiratory time between resting breathing and the highest loads L4 and L5. Significant differences were also found in inspiratory volume between resting breathing and all threshold loads, and between load L1 and loads L3-L5. These results indicate that the breathing strategies adopted during successive stages of the inspiratory threshold loading protocol were similar.

B. INVASIVE VS NONINVASIVE NMC

Fig. 4a-e show the relationships between electrical and mechanical measures of inspiratory muscle activity, measured both invasively ($fSEoesEMG_{di\%max}$ and $P_{di\%max}$ respectively) and noninvasively ($fSEsEMG_{lic\%max}$ and $fSE|sMMG_{lic}|_{\%max}$ respectively). Table 1 shows strong to very-strong correlations between $fSEoesEMG_{di\%max}$ and $P_{di\%max}$, $fSEsEMG_{lic\%max}$ and $P_{di\%max}$, and $fSEsEMG_{lic\%max}$ and $fSE|sMMG_{lic}|_{\%max}$.

The relationship between $fSEoesEMG_{di\%max}$ and $P_{di\%max}$ was more curvilinear than the relationships between $fSEsEMG_{lic\%max}$ and either $P_{di\%max}$ or $fSE|sMMG_{lic}|_{\%max}$. As explained in Appendix A, the relationship between $fSEoesEMG_{di\%max}$ and $P_{di\%max}$ is well described by an exponential model. Accordingly, iNMC (Fig. 4f) increased progressively and significantly from load L1 to load L5. In contrast, the relationships between $fSEsEMG_{lic\%max}$ and either $P_{di\%max}$ or $fSE|sMMG_{lic}|_{\%max}$ are well described by linear models, so that mNMCs (Fig. 4g and 4h) and nNMCs (Fig. 4i and 4j) increased very little, non-significantly, from load L1 to load L5. Table 2 shows individual linear regression results for iNMC, mNMC, and nNMC against inspiratory loads L1-L5. Statistically significant positive relationships were found between iNMC and inspiratory load (% PImax) in all subjects, in contrast to the absence of a significant relationship between mNMC or nNMC and inspiratory load in the majority of individuals studied.

IV. DISCUSSION AND CONCLUSION

The current gold standard assessment of diaphragm NMC in human subjects requires invasive measurements of P_{di} and oesEMG$_{di}$. These measurements are technically difficult and often uncomfortable for the individual being studied, presenting a barrier to the measurement of diaphragm
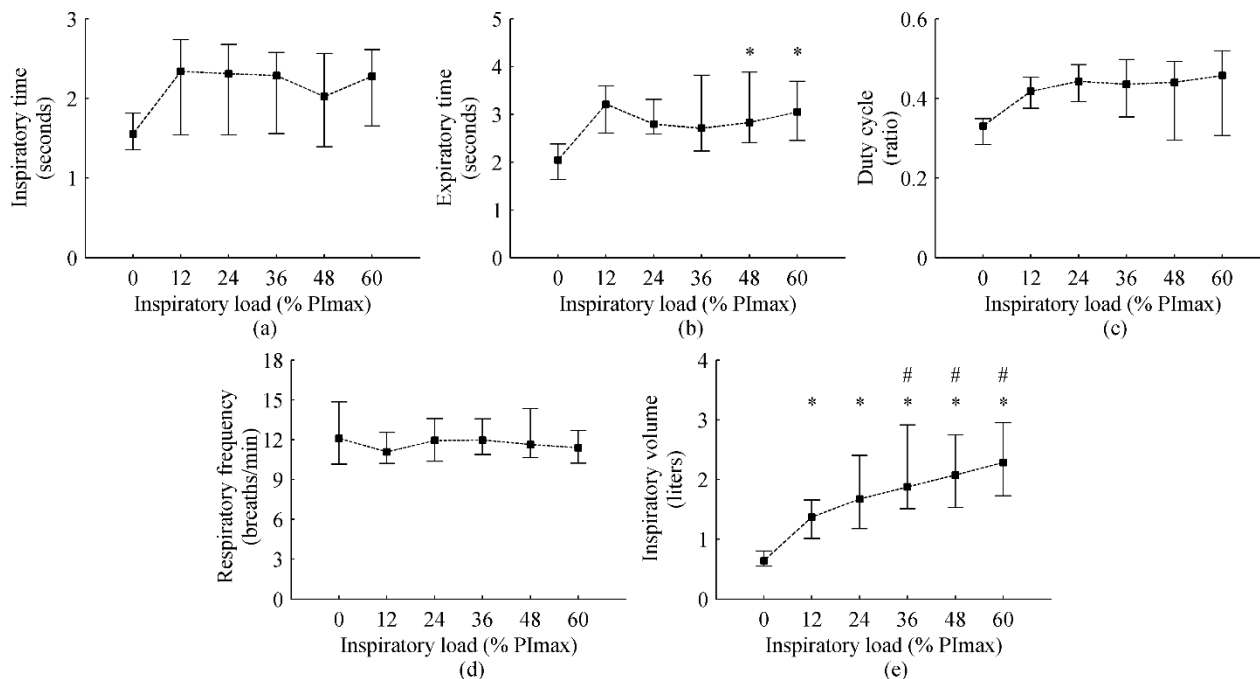
FIGURE 3. Evolution of inspiratory time, duty cycle, respiratory frequency, and inspiratory volume during progressive inspiratory threshold loading. Data points represent median and interquartile range of the 12 subjects for each load. Dashed black lines show the order of execution of the inspiratory threshold loads. Symbols * and # indicate statistically significant differences with respect to L0 (0% PImax) and L1 (12% PImax), respectively.

TABLE 1. Spearman's ρ between electrical and mechanical measures of inspiratory muscle activity.

Subject ID	$fSE_{oes}EMG_{di\%max}$-$P_{di\%max}$	$fSE_sEMG_{lic\%max}$ left-$P_{di\%max}$	$fSE_sEMG_{lic\%max}$ right-$P_{di\%max}$	$fSE_sEMG_{lic\%max}$ left-$fSE|sMMG_{lic|\%max}$ left	$fSE_sEMG_{lic\%max}$ right-$fSE|sMMG_{lic|\%max}$ right
1	0.85	0.95	0.92	0.81	0.89
2	0.94	0.94	0.93	0.84	0.88
3	0.80	0.82	0.84	0.94	0.91
4	0.77	0.90	0.93	0.90	0.94
5	0.90	0.96	0.89	0.94	0.89
6	0.80	0.84	0.84	0.89	0.84
7	0.76	0.96	0.96	0.94	0.96
8	0.71	0.97	0.97	0.95	0.94
9	0.93	0.96	0.96	0.93	0.93
10	0.64	0.78	0.81	0.89	0.83
11	0.57	0.73	0.76	0.79	0.76
12	0.89	0.88	0.86	0.87	0.91
Median (IQR)	0.80 (0.75-0.89)	0.92 (0.84-0.96)	0.90 (0.84-0.94)	0.90 (0.86-0.94)	0.90 (0.87-0.93)

NMC outside specialist research and clinical settings. This is the first study to compare measurements of diaphragm NMC using invasive techniques (the relationship between P_{di} and $oesEMG_{di}$) with noninvasive assessment of lower chest wall inspiratory muscle NMC using $sMMG_{lic}$ and $sEMG_{lic}$ measurements. Wholly noninvasive indices of lower chest wall inspiratory muscle NMC (nNMC, i.e., the ratio of $fSE|sMMG_{lic}|_{\%\,max}$ to $fSE_sEMG_{lic\%max}$) exhibited an immediate decrease at the onset of inspiratory loading (the transition from resting breathing to 12% PImax), followed by little and nonsignificant changes over progressive increases in inspiratory load between 12% and 60% of PImax. This is due to the mostly linear increase in $fSE|sMMG_{lic}|_{\%\,max}$

relative to $fSE_sEMG_{lic\%max}$ at increasing inspiratory loads. There was also a linear relationship between noninvasive $fSE_sEMG_{lic\%max}$ and invasive $P_{di\%max}$ measurements, again resulting in little change in mNMC with increasing inspiratory load. By contrast, the relationship between invasive $fSE_{oes}EMG_{di\%max}$ and $P_{di\%max}$ measurements was observed to be curvilinear, such that there was a progressive increase in iNMC with progressive increases in inspiratory threshold load.

Before considering these differences further, it is pertinent to review the key steps in the transformation of neural activation of the diaphragm, quantified as $oesEMG_{di}$, into P_{di}. The first step is translation of $oesEMG_{di}$ to muscle force, and
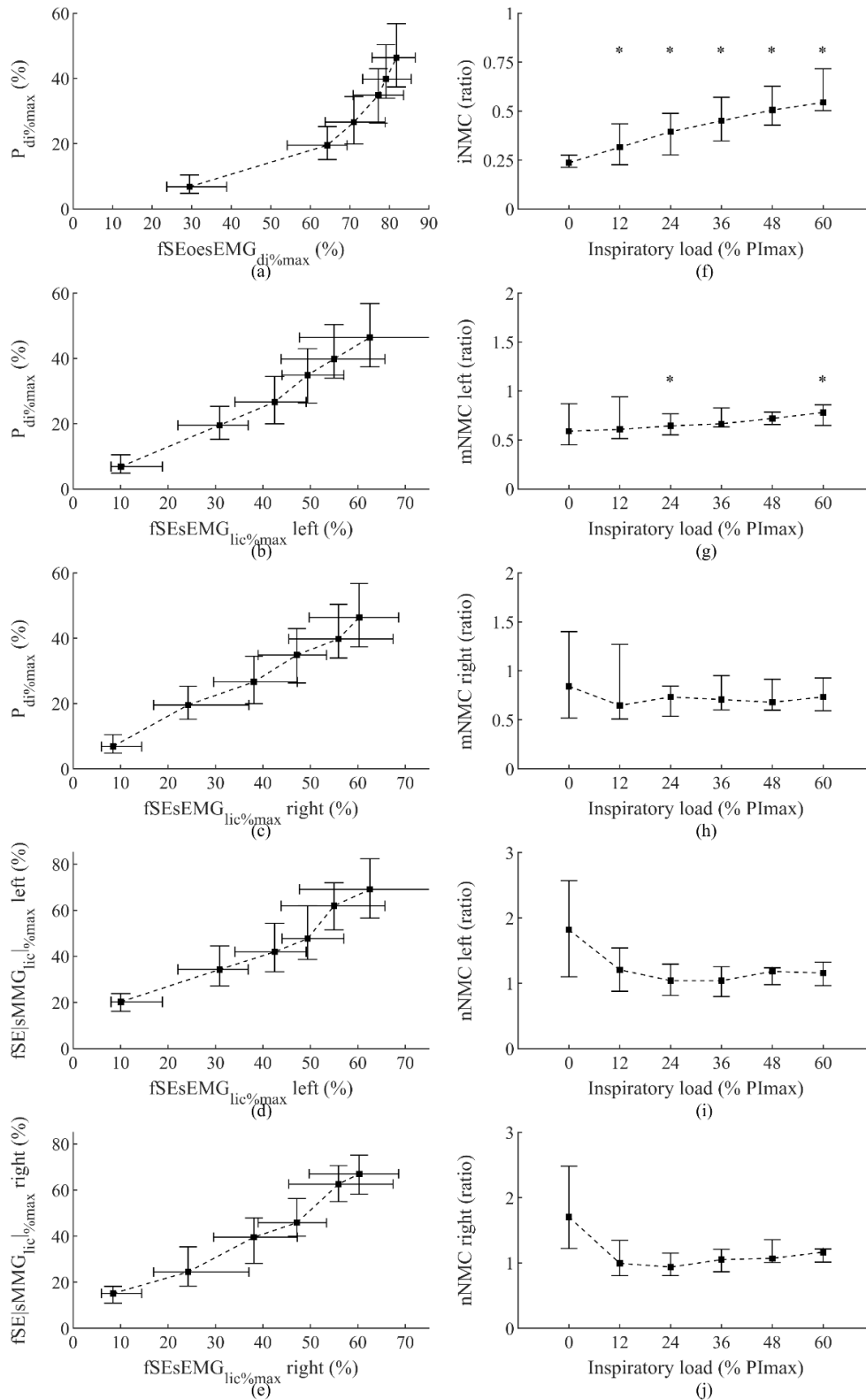
FIGURE 4. Relationship between electrical and mechanical measures of inspiratory muscle activation, and the corresponding NMC ratios, recorded during the incremental inspiratory threshold loading protocol. Invasive (iNMC), mixed (mNMC), and noninvasive (nNMC) NMCs were calculated as the ratios of $P_{di\%max}$ to $fSEoesEMG_{di\%max}$, $P_{di\%max}$ to $fSEsEMG_{lic\%max}$, and $fSE|sMMG_{lic}|_{\%max}$ to $fSEsEMG_{lic\%max}$, respectively. Data points represent median and interquartile range of the 12 subjects for each load. Dashed black lines show the order of execution of the inspiratory threshold loads. All data points with a ∗ symbol were significantly different to each other.

TABLE 2. Linear regression between NMCs and inspiratory loads L1-L5.

Subject ID	iNMC Slope	iNMC p value	mNMC left Slope	mNMC left p value	mNMC right Slope	mNMC right p value	nNMC left Slope	nNMC left p value	nNMC right Slope	nNMC right p value
1	0.067	0.002*	0.058	0.001*	0.052	0.077	0.040	0.603	0.060	0.185
2	0.063	0.027*	0.043	0.081	-0.061	0.273	0.004	0.917	0.126	0.175
3	0.057	0.043*	-0.119	0.212	-0.141	0.226	0.026	0.685	-0.098	0.160
4	0.053	0.024*	-0.003	0.892	-0.014	0.581	0.065	0.214	0.120	0.048*
5	0.060	0.010*	0.029	0.013*	0.004	0.095	0.024	0.301	0.138	0.032*
6	0.088	0.001*	0.017	0.734	-0.068	0.441	0.016	0.797	0.036	0.500
7	0.075	0.008*	-0.027	0.562	-0.024	0.501	-0.139	0.102	-0.046	0.018*
8	0.087	0.000*	0.041	0.144	0.035	0.043*	-0.043	0.192	-0.036	0.247
9	0.045	0.009*	0.045	0.053	-0.007	0.773	-0.117	0.236	-0.113	0.251
10	0.077	0.027*	0.041	0.373	0.029	0.500	0.039	0.330	0.037	0.389
11	0.063	0.001*	0.052	0.064	0.052	0.011*	0.019	0.784	0.050	0.099
12	0.046	0.012*	0.055	0.059	-0.003	0.949	-0.046	0.479	0.004	0.960

*Significant p values (<0.05)

the second is translation of diaphragm muscle force to P_{di}. As in other striated skeletal muscle, the relationship between oesEMG$_{di}$ and diaphragm force of contraction depends on the force-length, force-velocity, and force-frequency responses of the muscle [35]. Most or all of the reduction in P_{di} after increasing lung volume can be explained by the force-length properties of the diaphragm [36]. The relationship between diaphragm force and P_{di} depends on diaphragm curvature and chest wall (thoracoabdominal) configuration [37]. Grassino *et al.* observed that the slope of the relationship between crural oesEMG$_{di}$ and P_{di} during isometric diaphragmatic contractions at increasing lung volumes became steeper as ribcage and abdominal anteroposterior (AP) diameters decreased, indicating that the principal determinant of the gain in P_{di} relative to neural activation (i.e. the mechanical advantage of the diaphragm) at a given lung volume is thoracoabdominal configuration [37].

Observations of curvilinear relationships between fSEoesEMG$_{di\%max}$ and $P_{di\%max}$ in the present study are in keeping with previous work [38], [39]. Laghi *et al.* [39] attributed the apparent increased mechanical advantage of the diaphragm during inspiratory threshold loading to progressive increases in extradiaphragmatic muscle contribution to tidal breathing, expiratory muscle recruitment, and decreased end-expiratory lung volume. Expiratory muscle recruitment during inspiratory threshold loading decreases abdominal-wall compliance [40], and therefore may facilitate inspiration by increasing diaphragmatic length [41]. Decreased abdominal compliance can also increase the fulcrum effect of the abdominal contents on the diaphragm, thereby enhancing displacement/elevation of the lower ribcage by diaphragm contraction during inspiration [42]. Expiratory muscle recruitment has also been associated with progressive reductions in end-expiratory lung volume during inspiratory threshold loading, with consequent improvement in the mechanical advantage of the diaphragm [37], [38], [40], [43], [44]. Indeed, under conditions of increased ventilatory demand, increased mechanical output of the ribcage and abdominal muscles serves to optimize the mechanical advantage of the diaphragm by permitting the diaphragm to

operate at a greater overall length and limiting velocity of shortening [45].

In contrast to the curvilinear relationship between $P_{di\%max}$ and fSEoesEMG$_{di\%max}$, relationships between $P_{di\%max}$ and fSEsEMG$_{lic\%max}$, and fSE|sMMG$_{lic}|_{\%\,max}$ and fSEsEMG$_{lic\%max}$ were linear. Whereas oesEMG$_{di}$ signals are specific to the crural diaphragm [46], sEMG$_{lic}$ and sMMG$_{lic}$ signals recorded over the lower chest wall capture activation of the costal portion of the diaphragm [22] and are vulnerable to cross talk from extradiaphragmatic chest wall and abdominal muscle activation [20], [23], [24]. Although the diaphragm is the principal respiratory muscle engaged at rest [47], during increased ventilation [47] or inspiratory loading [48], [49], extradiaphragmatic muscle activity increases to allow the diaphragm to function under optimal length-tension characteristics [45]. Therefore, it is possible that the observation of a more linear relationship between $P_{di\%max}$ and fSEsEMG$_{lic\%max}$, and between fSE|sMMG$_{lic}|_{\%\,max}$ and fSEsEMG$_{lic\%max}$, than between $P_{di\%max}$ and fSEoesEMG$_{di\%max}$, results, in part, from progressive increases in extradiaphragmatic muscle activation serving to optimize the mechanical advantage of the diaphragm as inspiratory load increased. Crosstalk from extradiaphragmatic muscles would be expected to contribute to the sEMG$_{lic}$ and sMMG$_{lic}$ signals (and therefore to nNMC and mNMC), but not to oesEMG$_{di}$ or iNMC because the latter measures are specific to the diaphragm. An apparent "left-shift" in the relationship between $P_{di\%max}$ and fSEsEMG$_{lic\%max}$, when compared to the relationship between $P_{di\%max}$ and fSEoesEMG$_{di\%max}$ (Fig. 4), may also reflect greater neuromechanical efficiency of the costal vs crural diaphragm as recently demonstrated in a canine model [50].

An important advantage of this study is the use of fSampEn to analyze oesEMG$_{di}$, sEMG$_{lic}$ and |sMMG$_{lic}$| signals. These signals are highly contaminated by cardiac artefacts, which complicates the analysis especially using conventional RMS as in previous studies [19], [27], [29]–[31], [38], [39], [51]. Thus, an RMS-based analysis of myographic signals requires signal conditioning to reduce or eliminate cardiac

TABLE 3. Parameter estimates of the linear and exponential regression models to describe the relationships between electrical and mechanical measures of inspiratory muscle activity.

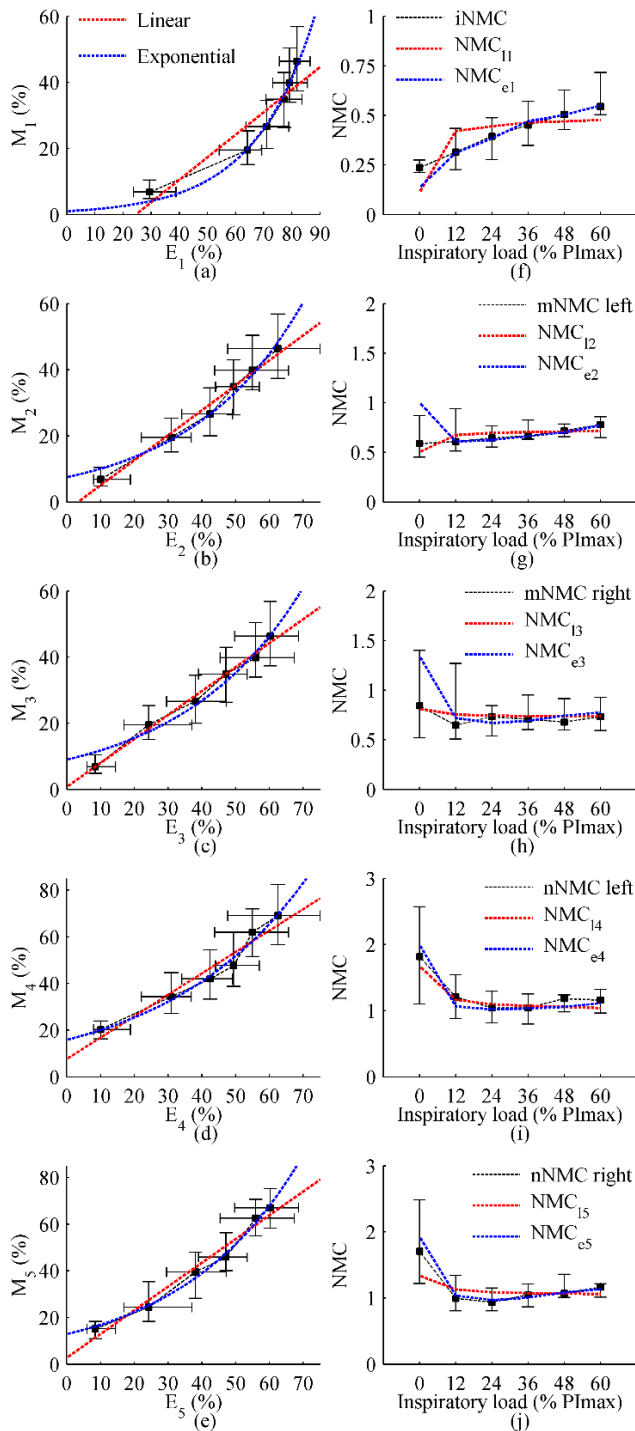|	Linear model					Exponential model				
	a_l	CI a_l	b_l	CI b_l	R^2	a_e	CI a_e	b_e	CI b_e	R^2
E_1=fSEoesEMG$_{di\%max}$ M_1=P$_{di\%max}$	0.68	(0.28, 1.08)	-16.75	(-44.40, 10.91)	0.85	1.03	(0.09, 1.96)	0.046	(0.034, 0.058)	0.99
E_2=fSEsEMG$_{lic\%max}$ left M_2=P$_{di\%max}$	0.76	(0.62, 0.89)	-2.53	(-8.60, 3.54)	0.98	7.48	(4.29, 10.66)	0.030	(0.022, 0.038)	0.98
E_3=fSEsEMG$_{lic\%max}$ right M_3=P$_{di\%max}$	0.72	(0.62, 0.83)	0.74	(-3.64, 5.12)	0.99	8.98	(4.71, 13.24)	0.027	(0.018, 0.036)	0.97
E_4=fSEsEMG$_{lic\%max}$ left M_4=fSE|sMMG$_{lic}$|$_{\%max}$ left	0.92	(0.60, 1.24)	7.59	(-6.83, 22.02)	0.94	15.81	(11.32, 20.29)	0.024	(0.018, 0.029)	0.98
E_5=fSEsEMG$_{lic\%max}$ right M_5=fSE|sMMG$_{lic}$|$_{\%max}$ right	1.02	(0.76, 1.28)	2.71	(-8.46, 13.88)	0.97	12.83	(9.85, 15.81)	0.028	(0.023, 0.032)	0.99

artefacts. However, fSampEn allows myographic signals to be analyzed with less interference from cardiac artefacts and without the need for prior rejection of cardiac artefacts. A combined analysis of sEMG$_{lic}$ and |sMMG$_{lic}$| using fSampEn would therefore allow NMC to be calculated noninvasively with minimal contamination by cardiac noise. Normalizing fSampEn of oesEMG$_{di}$, sEMG$_{lic}$ and |sMMG$_{lic}$| signals to that evoked during maximal volitional maneuvers provides measurements of the activity of inspiratory muscles relative to their capacity which are comparable between subjects. fSampEn-based measurements from inspiratory muscle myographic signals strongly correlate with the corresponding RMS-based measurements from the same signals, as described in previous studies [20], [21], [33]. Although both fSampEn and RMS can be used to analyze the amplitude of a signal, it is important to note, however, that fSampEn and RMS are conceptually different and, in fact, do not have the same units. Like RMS, fSampEn can track amplitude variations of a signal, and therefore can be used to estimate inspiratory muscle activation from myographic signals [21], [33]. However, fSampEn does not only depend on the amplitude, but also on the complexity of a signal. Therefore, fSampEn- and RMS-based measurements are not interchangeable.

The noninvasive nature of the sEMG$_{lic}$ and sMMG$_{lic}$ measurements is of potential value to clinical assessment of patients with cardiorespiratory and neuromuscular disease, as well as to future research studies of respiratory muscle function. The most powerful prognostic biomarker for mortality stratification in amyotrophic lateral sclerosis is twitch trans-diaphragmatic pressure [3]. The value of noninvasive indices of neuromechanical activation in patients with progressive neuromuscular disease is therefore worthy of further study. Increased neural respiratory drive, consequent to increased inspiratory muscle loading and neuromechanical uncoupling of the diaphragm, is strongly implicated in the perception of breathlessness and exercise limitation in

chronic respiratory disease [10], [52]–[55]. The development of noninvasive objective indices of NMC of the respiratory muscles would therefore be of value both to the clinical assessment of breathlessness patients, and mechanistic investigations of interventions that reduce breathlessness and increase exercise tolerance [56], [57].

We acknowledge the limitations of our study, which present opportunities for future investigation. Our study cohort was relatively small, comprising of twelve healthy subjects. The sample size reflects the challenges associated with recruitment to studies using invasive measures of diaphragm function. The potential clinical utility of noninvasive NMC measurements should be tested in disease populations such as COPD. The body mass index values of our participants were within the normal range. Since thicker layers of body fat act as attenuator filters for sMMG [58] and sEMG [59] signals, the effect of body composition and body mass index on the relationships between sMMG$_{lic}$ and sEMG$_{lic}$ measures in otherwise healthy individuals should be a focus of future research.

In conclusion, we have used 7th/8th intercostal space sEMG and sMMG recordings to derive noninvasive indices of lower chest wall inspiratory muscle NMC in healthy adults during an incremental inspiratory threshold loading protocol. In contrast to the significant increases in iNMC, derived as the ratio of P$_{di\%max}$ to fSEoesEMG$_{di\%max}$, there were little and nonsignificant changes in mNMC and nNMC during incremental inspiratory threshold loading, since the relationships between fSE|sMMG$_{lic}$|$_{\%\,max}$ and fSEsEMG$_{lic\%max}$, and P$_{di\%max}$ and fSEsEMG$_{lic\%max}$ were linear. We postulate that these differences may reflect increasing crosstalk from extradiaphragmatic lower chest wall and abdominal muscle activation to sEMG$_{lic}$ and sMMG$_{lic}$ signals (and hence to mNMC and nNMC), but not to crural oesEMG$_{di}$ signals and iNMC, the latter measures being specific to the diaphragm. Noninvasive indices of NMC derived from sEMG$_{lic}$ and

FIGURE 5. Linear (red) and exponential (blue) models fitted for the relationships between electrical and mechanical measures of inspiratory muscle activity. Black squares and bars represent median and interquartile range of the 12 subjects for each load.

$sMMG_{lic}$ may prove to be useful indices of lower chest wall inspiratory muscle NMC, particularly in settings that do not have access to invasive measures of diaphragm function.

APPENDIX
THEORETICAL EXPLANATION FOR THE EVOLUTION OF NMC DURING INSPIRATORY THRESHOLD LOADING

Inspiratory muscle NMC was calculated as the ratio of a mechanical measure to an electrical measure, and therefore the evolution of NMC during inspiratory threshold loading depends on the relationship between the measures involved in its calculation. The relationship between an electrical (E_i) and a mechanical (M_i) measure can be described in the simplest way by means of either a linear or an exponential function as in (A1) and (A2), respectively.

$$M_i = a_l \times E_i + b_l \tag{A1}$$

$$M_i = a_e \times e^{b_e \times E_i} \tag{A2}$$

where a_l, b_l, a_e, and b_e are the parameters of the models. The NMC, therefore, at a given level of inspiratory muscle electrical and mechanical activation can be expressed as in (A3) (linear case) and (A4) (exponential case).

$$EMC_l = \frac{M_i}{E_i} = a_l + \frac{b_l}{E_i} \tag{A3}$$

$$EMC_e = \frac{M_i}{E_i} = \frac{a_e \times e^{b_e \times E_i}}{E_i} \tag{A4}$$

According to (A3) and (A4), NMC_l and NMC_e values tend to be more dispersed for low values of E_i. However, NMC_l tends to a constant value (a_l) as E_i increases, whereas NMC_e increases.

Parameters of linear and exponential models were estimated using the median values of $fSEoesEMG_{di\%max}$ and $P_{di\%max}$, $fSEsEMG_{lic\%max}$ and $P_{di\%max}$, and $fSEsEMG_{lic\%max}$ and $fSE|sMMG_{lic}|_{\%\,max}$, of the 12 subjects for each load (see Table 3). Adjusted curves are shown together with data points in Fig. 5a-e. The relationship between $fSEoesEMG_{di\%max}$ and $P_{di\%max}$ was better described by the exponential model ($R^2 = 0.99$) than the linear model ($R^2 = 0.85$). However, the relationships between $fSEsEMG_{lic\%max}$ and either $P_{di\%max}$ or $fSE|sMMG_{lic}|_{\%\,max}$ were well described by both linear (R^2 ranging from 0.94 to 0.99) and exponential (R^2 ranging from 0.97 to 0.99) models, so the simplest model was selected, which was the linear model.

Theoretical NMCs were calculated using the estimated coefficients of linear and exponential models, as in (A3) and (A4). Fig. 5f-j show theoretical NMCs together with NMCs calculated using the acquired data. iNMC clearly increased with increasing load, so that it is better adjusted by the theoretical NMC derived from an exponential model. mNMC and nNMC, however, remained almost constant or increased slightly during threshold loads L1-L5, indicating that the relationships between $fSEsEMG_{lic\%max}$ and either $P_{di\%max}$ or $fSE|sMMG_{lic}|_{\%\,max}$ can be well explained by a linear model.

REFERENCES
[1] P. Laveneziana, "ERS statement on respiratory muscle testing at rest and during exercise," *Eur. Respir. J.*, vol. 53, no. 6, Jun. 2019, Art. no. 1801214.
[2] J. Steier, "The value of multiple tests of respiratory muscle strength," *Thorax*, vol. 62, no. 11, pp. 80–975, Nov. 2007.

[3] M. I. Polkey, R. A. Lyall, K. Yang, E. Johnson, P. Nigel Leigh, and J. Moxham, "Respiratory muscle strength as a predictive biomarker for survival in amyotrophic lateral sclerosis," *Amer. J. Respir. Crit. Care Med.*, vol. 195, no. 1, pp. 86–95, 2017.

[4] O. L. Wade, "Movements of the thoracic cage and diaphragm in respiration," *J. Physiol.*, vol. 124, no. 2, pp. 193–212, May 1954.

[5] J. Mead and S. H. Loring, "Analysis of volume displacement and length changes of the diaphragm during breathing," *J. Appl. Physiol.*, vol. 53, no. 3, pp. 750–755, Sep. 1982.

[6] C. M. Laroche, A. K. Mier, J. Moxham, and M. Green, "Diaphragm strength in patients with recent hemidiaphragm paralysis," *Thorax*, vol. 43, no. 3, pp. 170–174, Mar. 1988.

[7] A. J. Moore, J. Moxham, and M. I. Polkey, "Diaphragm weakness as a cause of breathlessness after anatomically distant surgery," *Thorax*, vol. 60, no. 9, pp. 786–787, Sep. 2005.

[8] J. Beck, "Electrical activity of the diaphragm during pressure support ventilation in acute respiratory failure," *Amer. J. Respir. Crit. Care Med.*, vol. 164, no. 3, pp. 419–424, 2001.

[9] M. I. Polkey, D. Kyroussis, C. H. Hamnegard, G. H. Mills, M. Green, and J. Moxham, "Diaphragm strength in chronic obstructive pulmonary disease," *Amer. J. Respir. Crit. Care Med.*, vol. 154, no. 5, pp. 1310–1317, Nov. 1996.

[10] D. E. O'Donnell, A. L. Hamilton, and K. A. Webb, "Sensory-mechanical relationships during high-intensity, constant-work-rate exercise in COPD," *J. Appl. Physiol.*, vol. 101, no. 4, pp. 1025–1035, Oct. 2006.

[11] D. E. O'Donnell, J. Ora, K. A. Webb, P. Laveneziana, and D. Jensen, "Mechanisms of activity-related dyspnea in pulmonary diseases," *Respir. Physiol. Neurobiol.*, vol. 167, no. 1, pp. 116–132, May 2009.

[12] A. Spinelli, G. Marconi, M. Gorini, A. Pizzi, and G. Scano, "Control of breathing in patients with myasthenia gravis," *Amer. Rev. Respir. Dis.*, vol. 145, no. 6, pp. 1359–1366, Jun. 1992.

[13] B. Lanini, "Perception of dyspnea in patients with neuromuscular disease," *Chest*, vol. 120, no. 2, pp. 402–408, Aug. 2001.

[14] M. Dres and A. Demoule, "Diaphragm dysfunction during weaning from mechanical ventilation: An underestimated phenomenon with clinical implications," *Crit. Care*, vol. 22, no. 1, p. 73, Mar. 2018.

[15] Y. M. Luo, J. Moxham, and M. I. Polkey, "Diaphragm electromyography using an oesophageal catheter: Current concepts," *Clin. Sci. (Lond)*, vol. 115, no. 8, pp. 233–244, Oct. 2008.

[16] C. Orizio and M. Gobbo, "Mechanomyography," in *Wiley Encyclopedia of Biomedical Engineering*. Hoboken, NJ, USA: Wiley 2006.

[17] L. Sarlabous, A. Torres, J. A. Fiz, J. Gea, J. M. Martínez-Llorens, and R. Jané, "Efficiency of mechanical activation of inspiratory muscles in COPD using sample entropy," *Eur. Respir. J.*, vol. 46, no. 6, pp. 1808–1811, 2015.

[18] L. Sarlabous, A. Torres, J. A. Fiz, J. M. Martínez-Llorens, J. Gea, and R. Jané, "Inspiratory muscle activation increases with COPD severity as confirmed by non-invasive mechanomyographic analysis," *PLoS One*, vol. 12, no. 5, May 2017, Art. no. e0177730.

[19] M. Petitjean and F. Bellemare, "Phonomyogram of the diaphragm during unilateral and bilateral phrenic nerve stimulation and changes with fatigue," *Muscle Nerve*, vol. 17, no. 10, pp. 1201–1209, Oct. 1994.

[20] M. Lozano-García, L. Sarlabous, J. Moxham, G. F. Rafferty, A. Torres, R. Jané, and C. J. Jolley, "Surface mechanomyography and electromyography provide non-invasive indices of inspiratory muscle force and activation in healthy subjects," *Sci. Rep.*, vol. 8, no. 1, p. 16921, Dec. 2018.

[21] L. Estrada, A. Torres, L. Sarlabous, and R. Jané, "Improvement in neural respiratory drive estimation from diaphragm electromyographic signals using fixed sample entropy," *IEEE J. Biomed. Health Inform.*, vol. 20, no. 2, pp. 476–485, Mar. 2016.

[22] D. Gross, A. Grassino, W. R. Ross, and P. T. Macklem, "Electromyogram pattern of diaphragmatic fatigue," *J. Appl. Physiol.*, vol. 46, no. 1, pp. 1–7, Jan. 1979.

[23] C. Sinderby, S. Friberg, N. Comtois, and A. Grassino, "Chest wall muscle cross talk in canine costal diaphragm electromyogram," *J. Appl. Physiol.*, vol. 81, no. 5, pp. 2312–2327, 1996.

[24] A. Demoule, E. Verin, C. Locher, J. P. Derenne, and T. Similowski, "Validation of surface recordings of the diaphragm response to transcranial magnetic stimulation in humans," *J. Appl. Physiol.*, vol. 94, no. 2, pp. 453–461, 2003.

[25] M. Yokoba, T. Abe, M. Katagiri, T. Tomita, and P. A. Easton, "Respiratory muscle electromyogram and mouth pressure during isometric contraction," *Respir. Physiol. Neurobiol.*, vol. 137, no. 1, pp. 51–60, Aug. 2003.

[26] A. H. Ramsook, "Diaphragm recruitment increases during a bout of targeted inspiratory muscle training," *Med. Sci. Sports Exerc.*, vol. 48, no. 6, pp. 1179–1186, 2016.

[27] C. C. Reilly, "Neural respiratory drive, pulmonary mechanics and breathlessness in patients with cystic fibrosis," *Thorax*, vol. 66, no. 3, pp. 240–246, Mar. 2011.

[28] A. Baydur, P. K. Behrakis, W. A. Zin, M. Jaeger, and J. Milic-Emili, "A simple method for assessing the validity of the esophageal balloon technique," *Amer. Rev. Respiratory Disease*, vol. 126, no. 5, pp. 788–791, 1982.

[29] Y. M. Luo and J. Moxham, "Measurement of neural respiratory drive in patients with COPD," *Respir. Physiol. Neurobiol.*, vol. 146, nos. 2–3, pp. 165–174, Apr. 2005.

[30] C. J. Jolley, "Neural respiratory drive in healthy subjects and in COPD," *Eur. Respir. J.*, vol. 33, no. 2, pp. 289–297, 2009.

[31] C. C. Reilly, C. J. Jolley, K. Ward, V. MacBean, J. Moxham, and G. F. Rafferty, "Neural respiratory drive measured during inspiratory threshold loading and acute hypercapnia in healthy individuals," *Exp. Physiol.*, vol. 98, no. 7, pp. 1190–1198, 2013.

[32] J. S. Richman and J. R. Moorman, "Physiological time-series analysis using approximate entropy and sample entropy," *Amer. J. Physiol.-Heart Circulatory Physiol.*, vol. 278, no. 6, pp. 2039–2049, 2000.

[33] L. Sarlabous, A. Torres, J. A. Fiz, and R. Jané, "Evidence towards improved estimation of respiratory muscle effort from diaphragm mechanomyographic signals with cardiac vibration interference using sample entropy with fixed tolerance values," *PLoS ONE*, vol. 9, no. 2, 2014, Art. no. e88902.

[34] M. Lozano-García, L. Estrada, and R. Jané, "Performance evaluation of fixed sample entropy in myographic signals for inspiratory muscle activity estimation," *Entropy*, vol. 21, no. 2, p. 183, Feb. 2019.

[35] D. F. Rochester, "The diaphragm: Contractile properties and fatigue," *J. Clin. Invest.*, vol. 75, no. 5, pp. 1397–1402, May 1985.

[36] M. J. Kim, W. S. Druz, J. Danon, W. Machnach, and J. T. Sharp, "Mechanics of the canine diaphragm," *J. Appl. Physiol.*, vol. 41, no. 3, pp. 369–382, Sep. 1976.

[37] A. Grassino, M. D. Goldman, J. Mead, and T. A. Sears, "Mechanics of the human diaphragm during voluntary contraction: Statics," *J. Appl. Physiol.*, vol. 44, no. 6, pp. 829–839, Jun. 1978.

[38] J. Beck, C. Sinderby, L. Lindström, and A. Grassino, "Effects of lung volume on diaphragm EMG signal strength during voluntary contractions," *J. Appl. Physiol.*, vol. 85, no. 3, pp. 1123–1134, Sep. 1998.

[39] F. Laghi, H. S. Shaikh, D. Morales, C. Sinderby, A. Jubran, and M. J. Tobin, "Diaphragmatic neuromechanical coupling and mechanisms of hypercapnia during inspiratory loading," *Respir. Physiol. Neurobiol.*, vol. 198, no. 1, pp. 32–41, 2014.

[40] P. R. Eastwood, D. R. Hillman, and K. E. Finucane, "Ventilatory responses to inspiratory threshold loading and role of muscle fatigue in task failure," *J. Appl. Physiol.*, vol. 76, no. 1, pp. 95–185, Jan. 1994.

[41] J. G. Martin and A. De Troyer, "The behaviour of the abdominal muscles during inspiratory mechanical loading," *Respir. Physiol.*, vol. 50, no. 1, pp. 63–73, Oct. 1982.

[42] W. S. Druz and J. T. Sharp, "Activity of respiratory muscles in upright and recumbent humans," *J. Appl. Physiol.*, vol. 51, no. 6, pp. 1552–1561, Dec. 1981.

[43] F. Laghi, M. J. Harrison, and M. J. Tobin, "Comparison of magnetic and electrical phrenic nerve stimulation in assessment of diaphragmatic contractility," *J. Appl. Physiol.*, vol. 80, no. 5, pp. 1731–1742, May 1996.

[44] A. De Troyer and T. A. Wilson, "Effect of acute inflation on the mechanics of the inspiratory muscles," *J. Appl. Physiol.*, vol. 107, no. 1, pp. 315–323, Jul. 2009.

[45] M. D. Goldman, A. Grassino, J. Mead, and T. A. Sears, "Mechanics of the human diaphragm during voluntary contraction: Dynamics," *J. Appl. Physiol.*, vol. 44, no. 6, pp. 840–848, Jun. 1978.

[46] J. Beck, C. Sinderby, L. Lindstrom, and A. Grassino, "Influence of bipolar esophageal electrode positioning on measurements of human crural diaphragm electromyogram," *J. Appl. Physiol.*, vol. 81, no. 3, pp. 1434–1449, Sep. 1996.

[47] G. Grimby, M. Goldman, and J. Mead, "Respiratory muscle action inferred from rib cage and abdominal V-P partitioning," *J. Appl. Physiol.*, vol. 41, no. 5, pp. 739–751, Nov. 1976.

[48] M. G. Sampson and A. De Troyer, "Role of intercostal muscles in the rib cage distortions produced by inspiratory loads," *J. Appl. Physiol.*, vol. 52, no. 3, pp. 517–523, Mar. 1982.

[49] P. M. Mengeot, J. H. Bates, and J. G. Martin, "Effect of mechanical loading on displacements of chest wall during breathing in humans," *J. Appl. Physiol.*, vol. 58, no. 2, pp. 477–484, Feb. 1985.

[50] G. Tagliabue, M. Ji, J. V. S. Jagers, D. J. Zuege, J. B. Kortbeek, and P. A. Easton, "Distinct neural-mechanical efficiency of costal and crural diaphragm during hypercapnia," *Respir. Physiol. Neurobiol.*, vol. 268, Jun. 2019, Art. no. 103247.

[51] L. Lin, L. Guan, W. Wu, and R. Chen, "Correlation of surface respiratory electromyography with esophageal diaphragm electromyography," *Respir. Physiol. Neurobiol.*, vol. 259, pp. 45–52, Jan. 2019.

[52] C. Sinderby, "Diaphragm activation during exercise in chronic obstructive pulmonary disease," *Amer. J. Respir. Crit. Care Med.*, vol. 163, no. 7, pp. 1637–1641, Jun. 2001.

[53] C. J. Jolley, Y. M. Luo, J. Steier, G. F. Rafferty, M. I. Polkey, and J. Moxham, "Neural respiratory drive and breathlessness in COPD," *Eur. Respir. J.*, vol. 45, no. 2, pp. 355–364, 2015.

[54] A. Faisal, "Common mechanisms of dyspnea in chronic interstitial and obstructive lung disorders," *Amer. J. Respir. Crit. Care Med.*, vol. 193, no. 3, pp. 299–309, Feb. 2016.

[55] C. J. Jolley and J. Moxham, "Dyspnea intensity: A patient-reported measure of respiratory drive and disease severity," *Amer. J. Respir. Crit. Care Med.*, vol. 193, no. 3, pp. 236–238, Feb. 2016.

[56] M. R. Schaeffer, "Neurophysiological mechanisms of exertional dyspnoea in fibrotic interstitial lung disease," *Eur. Respir. J.*, vol. 51, no. 1, Jan. 2018, Art. no. 103247.

[57] D. Langer, "Inspiratory muscle training reduces diaphragm activation and dyspnea during exercise in COPD," *J. Appl. Physiol.*, vol. 125, no. 2, pp. 381–392, Aug. 2018.

[58] E. M. Scheeren, "Influence of subcutaneous fat on mechanomyographic signals at three levels of voluntary effort," *Res. Biomed. Eng.*, vol. 32, no. 4, pp. 307–317, Jan. 2017.

[59] C. Nordander, "Influence of the subcutaneous fat layer, as measured by ultrasound, skinfold calipers and BMI, on the EMG amplitude," *Eur. J. Appl. Physiol.*, vol. 89, no. 6, pp. 514–519, Aug. 2003.

LUIS ESTRADA-PETROCELLI (M'08–SM'17) was born in Panama City, Panama, in 1982. He received the B.Sc. degree in biomedical engineering from the Universidad Latina de Panamá, Panama, in 2004, the M.Sc. degree in biomedical engineering from the Universitat de Barcelona and the Universitat Politècnica de Catalunya (UPC)-Barcelona Tech, Barcelona, Spain, in 2009, and the Ph.D. degree in biomedical engineering from UPC, in 2016. He is currently a Postdoctoral Researcher with the Institute for Bioengineering of Catalonia (IBEC), The Barcelona Institute of Science and Technology (BIST), and the Biomedical Research Networking Centre in Bioengineering, Biomaterials, and Nanomedicine (CIBER-BBN), Barcelona. He was a Research Fellow with the Department of Respiratory Medicine, King's College London, London, U.K., supported by a Long-Term Research Fellowship of the European Respiratory Society. His current research interests include signal processing techniques as well as the use of novel sensors and biomedical instrumentation for the evaluation of respiratory systems.

JOHN MOXHAM received the degree in economics from the London School of Economics (LSE), in 1967. He was a Research Fellow with LSE. He undertook his medical training with the University College Hospital, qualifying in 1973. His clinical training in general and respiratory medicine, including positions at the University College Hospital, Hammersmith Hospital, and Brompton Hospital. From 1977 to 1980, he was a Lecturer in medicine with the University College Hospital researching respiratory muscle physiology. In 1982, he was appointed as a Consultant Physician to the King's College Hospital and a Professor of respiratory medicine with the Faculty of Life Sciences and Medicine, King's College London, King's Health Partners, in 1990. For 30 years, his research interests have been respiratory physiology, including respiratory muscle weakness, neural respiratory drive, breathlessness, ventilatory failure, noninvasive intervention, and pulmonary rehabilitation, with over 350 authored and coauthored publications.

MANUEL LOZANO-GARCÍA was born in Barcelona, Spain, in 1983. He received the B.E. degree in telecommunications engineering and the M.S.E. and Ph.D. degrees in biomedical engineering from the Universitat Politècnica de Catalunya (UPC)-Barcelona Tech, Barcelona, in 2008, 2011, and 2016, respectively.

From 2011 to 2015, he was a Research Technician with the Institute for Bioengineering of Catalonia (IBEC), The Barcelona Institute of Science and Technology (BIST), and the Health Sciences Research Institute of the Germans Trias i Pujol Foundation. From 2015 to 2017, he was a Research Fellow with the King's College London. Since 2017, he has been a Postdoctoral Research Fellow with the Biomedical Research Networking Centre in Bioengineering, Biomaterials, and Nanomedicine (CIBER-BBN), IBEC, and since 2018, he has been an Associate Lecturer with the Department of Automatic Control, UPC. His research interests include biomedical signal acquisition, processing and interpretation. He particularly explores the use of noninvasive biomarkers of respiratory muscle and pulmonary function to improve the diagnosis and monitoring of patients with respiratory diseases.

Dr. Lozano-García was a recipient of the Long-Term Research Fellowship of the European Respiratory Society, in 2015. He also received the Special Doctoral Award by UPC, in 2018.

GERRARD F. RAFFERTY received the B.Sc. degree (Hons.) in physiology from the University of Leeds, U.K., and the Ph.D. degree in physiology from the King's College London, University of London, U.K.

He is currently a Reader in human and translational physiology with King's College London (KCL), Centre for Human and Applied Physiological Sciences within the School of Basic and Medical Biosciences, Faculty of Life Sciences and Medicine, and he is based in the Respiratory Muscle Laboratory, King's College Hospital. His research in the area of in vivo respiratory and peripheral muscle physiology across the life course in health and disease is internationally recognized and has published widely in this area with over 180 authored and coauthored publications. Working at the interface between basic and clinical physiology, his research has been translational, involving the development and further refinement of measurement techniques to allow understanding of basic physiological processes in healthy subjects and the effect of disease pathology and treatment interventions in patients.

ABEL TORRES (M'97–SM'19) was born in Figueres, Girona, Spain, in 1972. He received the M.Sc. degree in electrical engineering and the Ph.D. degree in biomedical engineering from the Universitat Politècnica de Catalunya (UPC)-Barcelona Tech, Barcelona, Spain, in 1997 and 2003, respectively. From 1998 to 2002, he worked as a Research Fellow with the Biomedical Engineering Research Centre (CREB), Barcelona. He is currently a Professor of automatic control with the Department of Automatic Control, UPC. He is also involved as a Senior Researcher with the Institute for Bioengineering of Catalonia (IBEC), The Barcelona Institute of Science and Technology (BIST), and the Biomedical Research Networking Center in Bioengineering, Biomaterials and Nanomedicine (CIBER-BBN). His primary interest focuses on the field of biomedical signal processing and its application to noninvasive analysis of respiratory muscle signals.

CAROLINE J. JOLLEY received the M.A. degree (Hons.) in medical and veterinary sciences tripos from the University of Cambridge, the M.B.B.S. degree in clinical medicine from the King's College School of Medicine and Dentistry, London, U.K., and the Ph.D. degree from the King's College London, University of London, U.K., in 2012. She is currently a Senior Lecturer in human physiology with the Centre for Human and Applied Physiology, Faculty of Life Sciences and Medicine, School of Basic and Medical Biosciences King's College London. She also works as a Consultant in respiratory medicine with the King's College Hospital NHS Foundation Trust, King's Health Partners. Her principal research interest is the use of measurements of respiratory muscle function and neural respiratory drive to investigate the physiological basis of breathlessness and respiratory failure in cardiorespiratory and neuromuscular disease.

RAIMON JANÉ (M'91–SM'14) received the Ph.D. degree from the Universitat Politècnica de Catalunya (UPC)-Barcelona Tech, Barcelona, Spain, in 1989. He is currently the Director of Research with the Department of Automatic Control, UPC, and the Scientific Group Leader of the Biomedical Signal Processing and Interpretation Group, Institute for Bioengineering of Catalonia (IBEC), The Barcelona Institute of Science and Technology (BIST), Barcelona. Since 2008, he has been the Principal Investigator of the Biomedical Signals and Systems (SISBIO) Group and a member of the Steering Committee of the Biomedical Research Networking Centre, Bioengineering, Biomaterials, and Nanomedicine (CIBER-BBN). He is also a Professor of the master's degree programme and the Coordinator of the Ph.D. programme in biomedical engineering with UPC. His research interests include multimodal and multiscale biomedical signal processing in cardiorespiratory diseases and sleep disorders. In 2005, he received the Barcelona City Prize from the Barcelona City Council in technology research. He is a member of the IEEE EMBS Technical Committee on Cardiopulmonary Systems and an Associate Editor of the Cardiovascular and Respiratory Systems Engineering Theme of the IEEE EMBC. He has been the President of the Spanish Society of Biomedical Engineering (SEIB), since 2012.

● ● ●